Fluorescence Ratio Imaging

Geert M.P. van Kempen, Lucas J. van Vliet, Robert P.W. Duin

Pattern Recognition Group of the Faculty of Applied Physics
Delft University of Technology
Lorentzweg 1, 2628 CJ Delft, The Netherlands

e-mail: geert@ph.tn.tudelft.nl

Abstract
In this paper, the properties of the mean and variance of three estimators of the ratio between two random variables *x*, *y* are discussed. Given *n* samples of *x* and *y* we can construct two different estimators. One is biased and the other is asymptotically unbiased. Using the noise characteristics (variance, covariance) a third, unbiased estimator can be constructed.

1. Introduction

In fluorescence microscopy, ratio imaging is applied in a number of applications. In ratio labeling, the ratio between the intensities of different fluorochromes is used to expand the number of labels for an in situ hybridization procedure [1]. This number is normally restricted by the number of fluorochromes that can be spectrally separated by fluorescence microscopy.

Fluorescence ratio imaging is also used to measure spatial and temporal differences in ion concentrations within a single cell. This is achieved by using fluorochromes whose excitation or emission spectrum change as function of the Ca^{++} or pH concentration [2].

In a third application of ratio imaging, known as Comparative Genome Hybridization (CGH) [3,4], one tries to estimate the DNA sequence copy number as a function of the chromosomal location. This is achieved by measuring the ratio between "tumor" DNA and "normal" DNA to detect gene amplifications and deletions.

In fluorescence ratio imaging, one is interested in the ratio *R* between two random variables *X* and *Y*,

$$R = \frac{X}{Y} \tag{1}$$

In practice, one can not measure *X* and *Y*, but only "noisy" realizations of *X* and *Y*, named *x* and *y* in this paper. We will assume *x* and *y* to be stochastic variables with $\mathrm{E}\{x\} = \mu_x = X$ and $\mathrm{E}\{y\} = \mu_y = Y$. In section 2 we study the statistical properties of two estimators of the ratio *R*. Based on these results we show in section 3 that under certain conditions (known variance, covariance) a third, unbiased estimator can be constructed. The variance of this unbiased estimator is compared in section 4 with the Cramer-Rao lower bound. The theory will be supported by simulations and experiments which are described in section 5. In section 6, we discuss two applications of ratio imaging in fluoresence microscopy.

2. The mean and variance of two ratio estimators

Given *n* samples of *x* and *y* we can obtain two different estimators for the ratio *R*= *X*/*Y*:

$$r_1 = \frac{\bar{x}}{\bar{y}} \qquad\qquad r_2 = \overline{\left(\frac{x}{y}\right)} \tag{2}$$

G.M.P. van Kempen, L.J. van Vliet, and R.P.W. Duin, Fluorescence ratio imaging, in: J. Van Katwijk, J.J. Gerbrands, M.R. van Steen, J.F.M. Tonino (eds.), ASCI'95, Proc. First Annual Conf. of the Advanced School for Computing and Imaging (Heijen, NL, May 16-18), ASCI, Delft, 1995, 233-242.

To find an approximate expression for the expectation of r_1 and r_2, we have used a Taylor series expansion of x/y (or $\bar{x}/\bar{y}$) around μ_X, μ_Y,

$$\begin{aligned}\frac{x}{y} \approx & \left.\frac{x}{y}\right|_{\mu_x,\mu_y} + (x-\mu_x)\left.\frac{\partial}{\partial x}\left(\frac{x}{y}\right)\right|_{\mu_x,\mu_y} + (y-\mu_y)\left.\frac{\partial}{\partial y}\left(\frac{x}{y}\right)\right|_{\mu_x,\mu_y} \\ & + \frac{1}{2!}(x-\mu_x)^2\left.\frac{\partial^2}{\partial x^2}\left(\frac{x}{y}\right)\right|_{\mu_x,\mu_y} + \frac{1}{2!}(y-\mu_y)^2\left.\frac{\partial^2}{\partial y^2}\left(\frac{x}{y}\right)\right|_{\mu_x,\mu_y} \\ & + (x-\mu_x)(y-\mu_y)\left.\frac{\partial^2}{\partial x\partial y}\left(\frac{x}{y}\right)\right|_{\mu_x,\mu_y} + O\left(\left((x-\mu_x)\frac{\partial}{\partial x}+(y-\mu_y)\frac{\partial}{\partial y}\right)^3\left(\frac{x}{y}\right)\right)\end{aligned} \tag{3}$$

We ignore all high order terms (terms higher than two). A Taylor series expansion of $\bar{x}/\bar{y}$ around μ_X, μ_Y is similar to eq. 3. The mean of r_1 and r_2 can be found by applying the expectation operator to the individual terms,

$$\mathrm{E}\{r_1\} = \mathrm{E}\left\{\frac{\bar{x}}{\bar{y}}\right\} \approx \frac{\mu_x}{\mu_y} + \mathrm{var}(\bar{y})\frac{\mu_x}{\mu_y^3} - \frac{\mathrm{cov}(\bar{x},\bar{y})}{\mu_y^2} \approx \frac{\mu_x}{\mu_y} + \frac{1}{n}\left(\mathrm{var}(y)\frac{\mu_x}{\mu_y^3} - \frac{\mathrm{cov}(x,y)}{\mu_y^2}\right) \tag{4a}$$

and

$$\mathrm{E}\{r_2\} = \mathrm{E}\left\{\overline{\left(\frac{x}{y}\right)}\right\} = \mathrm{E}\left\{\frac{x}{y}\right\} \approx \frac{\mu_x}{\mu_y} + \mathrm{var}(y)\frac{\mu_x}{\mu_y^3} - \frac{\mathrm{cov}(x,y)}{\mu_y^2} \tag{4b}$$

It is clear from these two expressions that r_1 is asymptotically unbiased (lim $n\to\infty$ E{r_1} = μ_x/μ_y), and that r_2 is a biased estimator or *R*. An approximation of the variance of r_1 and r_2 is obtained using the first order terms of the Taylor series expansion.

$$\begin{aligned}\mathrm{var}(r_1) = \mathrm{var}\left(\frac{\bar{x}}{\bar{y}}\right) &= \mathrm{E}\left\{\left(\frac{\bar{x}}{\bar{y}} - \mathrm{E}\left\{\frac{\bar{x}}{\bar{y}}\right\}\right)^2\right\} \approx \mathrm{E}\left\{\left(\frac{\bar{x}}{\bar{y}} - \frac{\mu_x}{\mu_y}\right)^2\right\} \\ &\approx \frac{\mathrm{var}\,\bar{x}}{\mu_y^2} + \frac{\mu_x^2\,\mathrm{var}\,\bar{y}}{\mu_y^4} - \frac{2\mu_x\,\mathrm{cov}(\bar{x},\bar{y})}{\mu_y^3} \approx \frac{1}{n}\left(\frac{\mathrm{var}\,x}{\mu_y^2} + \frac{\mu_x^2\,\mathrm{var}\,y}{\mu_y^4} - \frac{2\mu_x\,\mathrm{cov}(x,y)}{\mu_y^3}\right)\end{aligned} \tag{5a}$$

and

$$\begin{aligned}\mathrm{var}(r_2) = \mathrm{var}\left(\overline{\left(\frac{x}{y}\right)}\right) = \frac{1}{n}\mathrm{var}\left(\frac{x}{y}\right) &= \frac{1}{n}\mathrm{E}\left\{\left(\frac{x}{y} - \mathrm{E}\left\{\frac{x}{y}\right\}\right)^2\right\} \approx \frac{1}{n}\mathrm{E}\left\{\left(\frac{x}{y} - \frac{\mu_x}{\mu_y}\right)^2\right\} \\ &\approx \frac{1}{n}\left(\frac{\mathrm{var}\,x}{\mu_y^2} + \frac{\mu_x^2\,\mathrm{var}\,y}{\mu_y^4} - \frac{2\mu_x\,\mathrm{cov}(x,y)}{\mu_y^3}\right)\end{aligned} \tag{5b}$$

Estimators r_1 and r_2 have, only in first order Taylor series expansion, an equal variance, which both diminish for an infinite number of samples ($n\to\infty$). Therefore, both estimators r_1 and r_2 are consistent. Furthermore, the variance and bias of both estimators is smallest when the random variable with the largest mean is placed in the denominator. An expression, similar to equations (5), for the variance of x/y was found by Kendall and Stuart [5].

3. An unbiased ratio estimator

In the previous section, we found that the estimator r_1 is only asymptotically unbiased. However, having found an analytical expression of the bias, we can derive a unbiased estimator for R based on r_1,

$$r_3 = \frac{\bar{x}}{\bar{y}} - \frac{1}{n}\left(\frac{\mu_x}{\mu_y^3}\operatorname{var} y - \frac{\operatorname{cov}(x,y)}{\mu_y^2}\right) \tag{6}$$

The expectation for this estimator is, of course,

$$\mathrm{E}\{r_3\} = \mathrm{E}\left\{\frac{\bar{x}}{\bar{y}} - \frac{1}{n}\left(\frac{\mu_x}{\mu_y^3}\operatorname{var} y - \frac{\operatorname{cov}(x,y)}{\mu_y^2}\right)\right\} \approx \frac{\mu_x}{\mu_y} \tag{7}$$

The variance of this estimator yields,

$$\operatorname{var}(r_3) = \mathrm{E}\left\{\left(\frac{\bar{x}}{\bar{y}} - \mathrm{E}\left\{\frac{\bar{x}}{\bar{y}}\right\}\right)^2\right\} = \operatorname{var}(r_1) \tag{8}$$

The estimator r_3 is an unbiased estimator of R with a variance equal to the variance of r_1.

With a similar argument as used before in this section, we can derive an unbiased estimator based on r_2,

$$r_4 = \overline{\left(\frac{x}{y}\right)} - \left(\frac{\mu_x}{\mu_y^3}\operatorname{var} y - \frac{\operatorname{cov}(x,y)}{\mu_y^2}\right) \tag{9}$$

Ratio estimator r_4 is less meaningful than r_3. The precision and accuracy of the bias term directly influences the correction term of estimator r_4. In practice we have to estimate μ_x, μ_y and var y from the same n samples. Note that the bias term of r_3 is divided by the number of samples n. Therefore an error made in estimating the bias term has less influence on ratio estimator r_3 than r_4.

4. Cramer-Rao lower bound

Assuming Gaussian distributed realizations of x and y. The joint probability density function is given by

$$f(\mathbf{w},\boldsymbol{\mu}) = \prod_{i=1}^{n} \frac{1}{2\pi|\boldsymbol{\Sigma}|^{\frac{1}{2}}} \exp\left(-\tfrac{1}{2}(\mathbf{w}_i - \boldsymbol{\mu})^{\mathbf{T}} \boldsymbol{\Sigma}^{-1}(\mathbf{w}_i - \boldsymbol{\mu})\right) \tag{10}$$

with $\mathbf{w}_i = (x_i, y_i)$, and $\boldsymbol{\mu} = (\mu_x, \mu_y)$. Given an unbiased estimator r, the Cramer-Rao lower bound (CRLB) is given by

$$\operatorname{var}(r) \geq \left(\frac{\partial R}{\partial \boldsymbol{\mu}}\right)\left(-E\left\{\frac{\partial^2 \ln f(\mathbf{w},\boldsymbol{\mu})}{\partial \boldsymbol{\mu}^2}\right\}\right)^{-1}\left(\frac{\partial R}{\partial \boldsymbol{\mu}}\right)^{\mathbf{T}} \tag{11}$$

This yields the minimum variance bound for all unbiased ratio estimators

$$\operatorname{var}(r) \geq \frac{1}{n}\left(\frac{1}{\mu_y^2}\operatorname{var} x + \left(\frac{\mu_x}{\mu_y^2}\right)^2 \operatorname{var} y - \frac{2\mu_x}{\mu_y^3}\operatorname{cov}(x,y)\right) \tag{12}$$

Now we can compare the variance of all unbiased ratio estimators with the CRLB. The variance of the unbiased ratio estimator r_3 is equal to this lower bound.

5. Experiments

Some simulations were performed to support the expressions for the mean and variance of r_1, r_2 and r_3. In the first experiment we used computer generated noise whereas in the second experiment we used noise images generated in fluorescence image acquisition.

5.1. *Simulations*

An image of size *nxm* was filled with realizations of *x*, N(μ_x,σ_x) (Numerical Recipes [6]) and another image was filled with realizations of *y*, N(μ_y,σ_y). Figure 1 shows the mean and variance of r_1, r_2 and r_3 as a function of the number of samples *n*. Note that r_1 asymptotically converges to μ_x/μ_y, r_2 remains biased even for large values of *n*, whereas r_3 is unbiased even for small number of samples. The means of r_1 and r_3 are in agreement with the predictions whereas the mean of r_2 converges to a slightly higher ratio than predicted using a second order Taylor approximation as in eq. 4b. The estimated variance of r_1 and r_3 are in agreement with the theoretical variances as derived in section 2. The estimated variance of r_2 is larger than we had expected from our calculations using only a first order Taylor approximation.

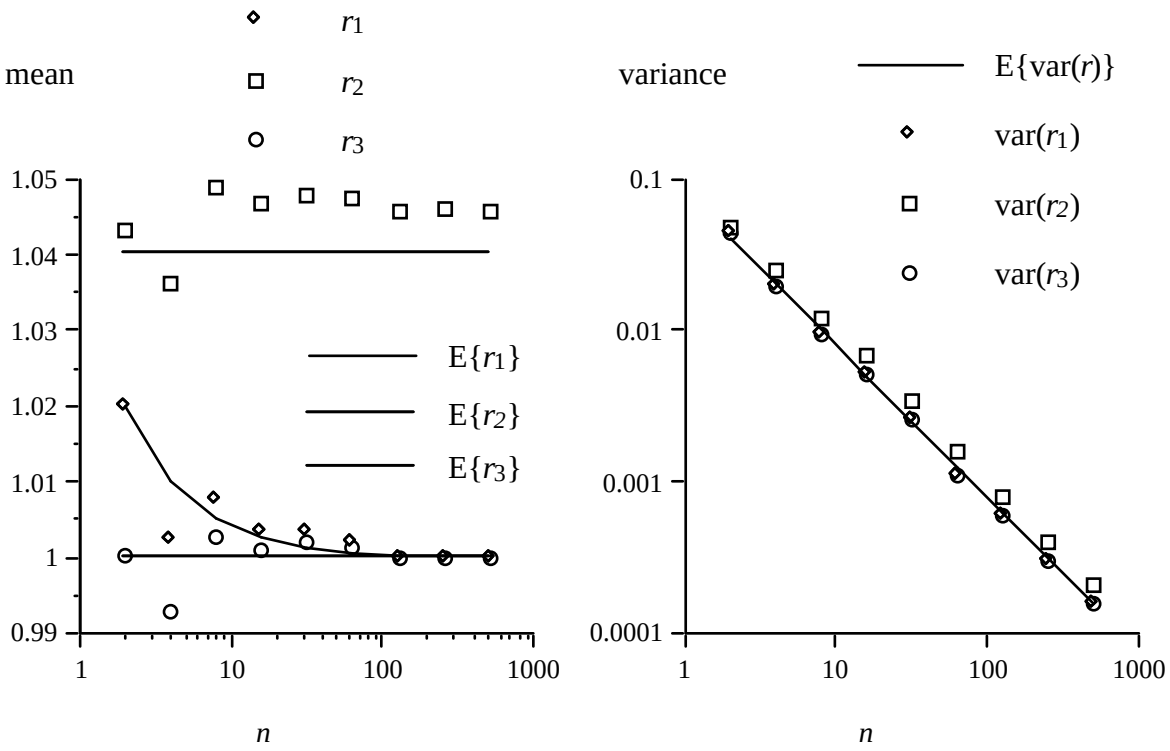

Figure 1: The mean and variance of r_1 and r_2 measured as a function of *n*, with $\mu_x = \mu_y =$ 40.0 and $\sigma_x = \sigma_y = 8.0$. Each point is an average of 1024 realizations.

5.2. *Experiments in Practice*

To test the presented theory in practice we performed the following experiment. An image was acquired of a homogenous illuminated scene. The acquired data is disturbed by several noise sources:

- photon shot noise (Poisson noise due to the counting of electrons induced by single photons),
- readout noise (Gaussian noise caused by the pre-amplifier),
- quantization noise (uniform noise caused by analog-to-digital conversion),
- dark current (very small, Poisson distributed signal),
- bias, space dependent offset signal.

If we acquire a second image of the same scene and subtract the two we are left with a noise image of zero mean and twice the variance. This can be repeated to produce a second independent noise image. Both noise images can be added to a constant valued image after which the ratio estimators r_1, r_2 and r_3 can be applied. Noise images acquired this way, will contain photon shot noise, readout noise and quantization noise.

Figure 2 shows the mean and variance of the ratio of the two noise images, as estimated by the three estimators r_1, r_2 and r_3 as a function of the number of samples n.

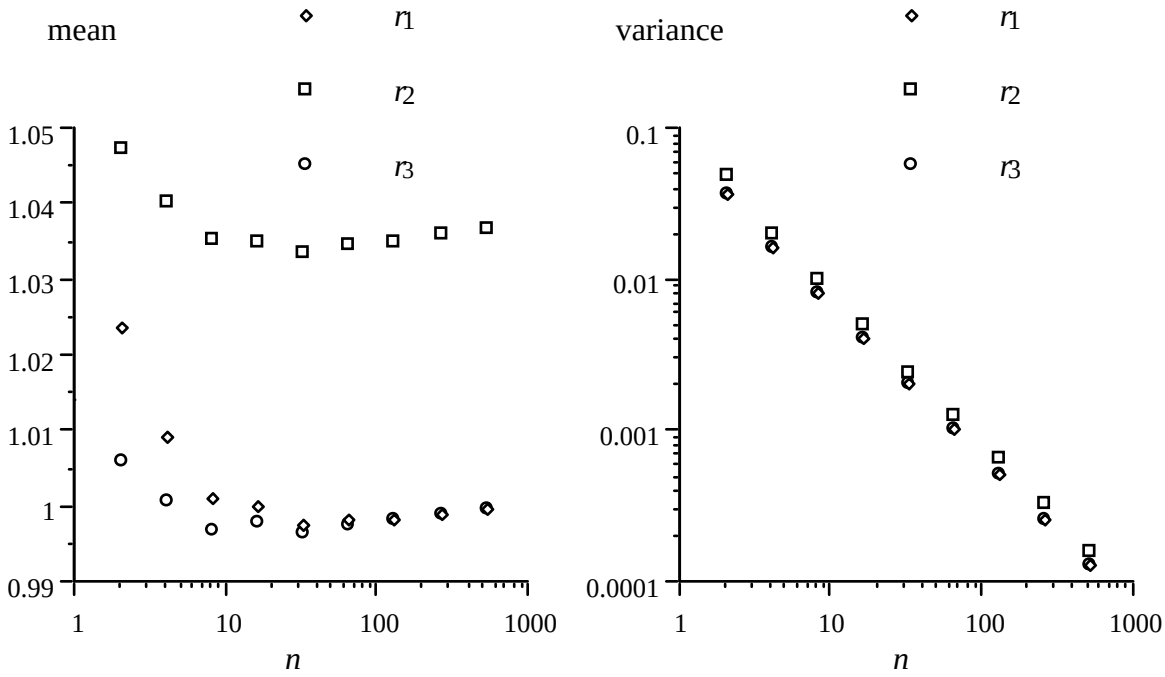

Figure 2: The mean and variance of r_1, r_2 and r_3 measured as a function of n. The mean value of the two noise images were set to 100.0, the variances of both images are 328.84 and 329.37.

6. Applications in Fluorescence Microscopy

We will discuss two applications in quantitative fluorescence microscopy that are based on ratio imaging. The first compares the genome of tumor cells with that of a healthy normal to detect numerical aberrations of specific genes. The second uses ratio labels to identify whole chromosomes or specific chromosomal targets. The use of ratio labels increases the number of task that can be done simultaneously.

6.1. *Improved statistics on ratio profiles*

Comparative Genome Hybridization (CGH) [3,4] estimates the DNA sequence copy number as function of the chromosomal location. This is achieved by ratio imaging of “tumor” DNA and “normal” DNA to detect gene amplifications and deletions. To improve the precision and accuracy of such a ratio profile, it is common practice in CGH analysis, to average over a

number of ratio profiles of the same chromosome. If we call this ratio estimator r_{mn}, we can write it as,

$$r_{mn} = \frac{1}{m}\sum_{j=1}^{m}\left\{\frac{1}{n}\sum_{i=1}^{n}x_i \Big/ \frac{1}{n}\sum_{i=1}^{n}y_i\right\} = \frac{1}{m}\sum_{j=1}^{m}\left\{\frac{\bar{x}}{\bar{y}}\right\} \tag{13}$$

where m is the number of profiles, and n the number of x, y values at a certain position on each profile. Equation (13) shows that estimator r_{mn} is identical to applying estimator r_1 m times on n samples followed by averaging over the obtained m ratios. An approximation of the expectation of r_{mn} can be found using a second order Taylor series expansion,

$$\mathrm{E}\{r_{mn}\} = \mathrm{E}\left\{\frac{1}{m}\sum_{j=1}^{m}\left\{\frac{1}{n}\sum_{i=1}^{n}x_i \Big/ \frac{1}{n}\sum_{i=1}^{n}y_i\right\}\right\} = \mathrm{E}\left\{\frac{1}{n}\sum_{i=1}^{n}x_i \Big/ \frac{1}{n}\sum_{i=1}^{n}y_i\right\} = \mathrm{E}\{r_1\} \tag{14}$$

The variance of r_{mn} can be approximated by a first order Taylor series expansion to obtain

$$\mathrm{var}(r_{mn}) = \frac{1}{m}\mathrm{E}\left\{\left(\frac{\bar{x}}{\bar{y}} - \mathrm{E}\left\{\frac{\bar{x}}{\bar{y}}\right\}\right)^2\right\} = \frac{1}{m}\mathrm{var}(r_1) \tag{15}$$

The expressions for the mean and variance of r_{mn} (eqs. (14,15)) show that averaging over ratio profiles only improves the precision of the estimation of R. It does not improve the accuracy.

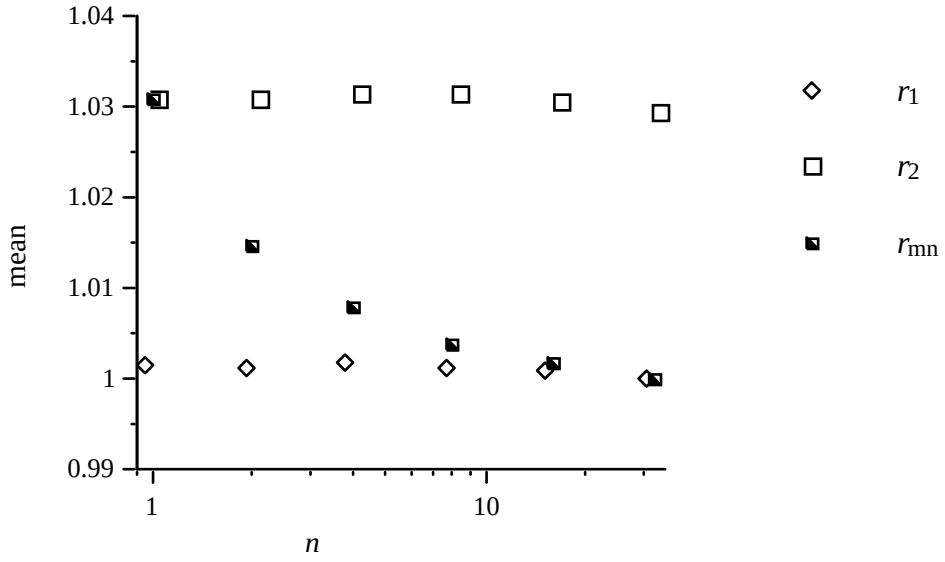

Figure 3: The mean of r_{mn}, r_1 and r_2 measured as function of n, with a constant number of samples divided over m and n in such a way that m x n = 32, $\mu_x = \mu_y = 36.0$ and $\sigma_x = \sigma_y = 6.0$.

A simulation experiment was performed to compare the performance of estimator r_{mn} with r_1 and r_2 for a constant number of $m \times n$ samples. Again two images were filled with Gaussian distributed noise, and the ratios between both images were estimated using r_{mn}, r_1 and r_2. The mean and variance of r_{mn} were calculated as function of the ratio between n and m, the mean and variance of r_1 and r_2 were calculated from $m \times n$ samples.

Figure 3 shows the results of an experiment with r_{mn}, r_1 and r_2 where $m \times n$ equals 32 samples. Note that estimator r_1 has already converged for this number of samples (see also

figure 1). It is clear that estimator r_{mn} yields a suboptimal estimation of the ratio for a given number of $m \times n$ samples. This shows again that averaging before taking the ratio yields a better ratio estimate.

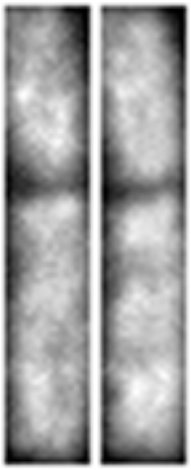

Figure 4: CGH image of a chromosome 2. The "normal" or "reference" DNA is labeled with FITC (left image) and the "tumor" or "unknown" DNA is labeled with Texas Red (right image).

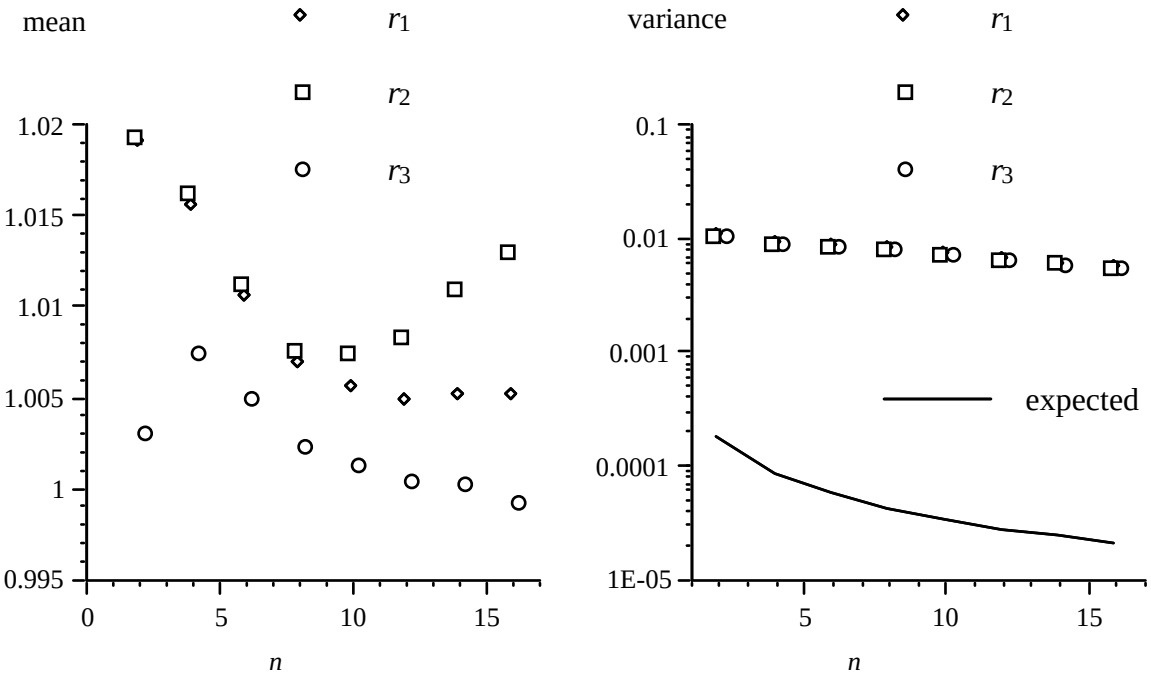

Figure 5: The mean of r_1, r_2 and r_3 measured as function of n. The mean values were estimated over 86 realizations. The measured variances are two orders of magnitude higher than can be expected from the characteristics of the image acquisition system [7].

In another experiment, we used CGH control images to verify whether the differences between estimators r_1, r_2 and r_3 could be found on real data. These CGH control images are made using normal DNA for both test and reference DNA, thus after calibration a ratio of 1.0 is to be expected. From a set of CGH images, we selected a straight, vertically oriented chromosome (figure 4), to avoid errors due to resampling and straightening of the chromosome pixel data. A small neighborhood region around the chromosome was used to estimate a constant

background intensity, which was subtracted from the chromosome intensity values. To correct for the different chromatic efficiencies of the color filters and camera used, the intensity of the two CGH signals of the chromosome were scaled such that the average intensity were equal.

The CGH images were acquired using a Photometrics camera with a KAF1400 chip with an electronic gain of 1 [4]. From noise measurements with this camera [7], we can estimate the variance on the ratio estimation induced by the image acquisition, and compare this with the measured variance.

We calculated the mean and variance of r_1, r_2 and r_3 from a region of interested, with size n, which was centered around the middle of both the images. Figure 5 shows the mean values of the three estimators as a function of the number of samples n, taken in the horizontal direction of the image (figure 4). The mean and variance were estimated over 86 realizations (the vertical dimension of the image is 86 pixels). Figure 5 also shows the variances of r_1, r_2 and r_3 as a function of the number of samples n. We estimated the expected acquisition variance to be in the order of 10^{-4}, assuming a photon limited behavior of the camera and using an average intensity of the chromosome data of 800 ADU (Analog-to-Digital Units). Figure 5 clearly shows that the variances of the ratio estimators is dominated by variations of the image due to variations in biology and sample preparation, and not by the noise of the imaging system. The increase of the bias of estimator r_2 for values of n larger then 10, are caused by a decrease of the signal-to-noise ratio at the edges of the chromosome. In figure 6 the estimated bias terms of r_1 and r_2 are plotted. The bias of r_2 is a factor n times larger than the bias of r_1.

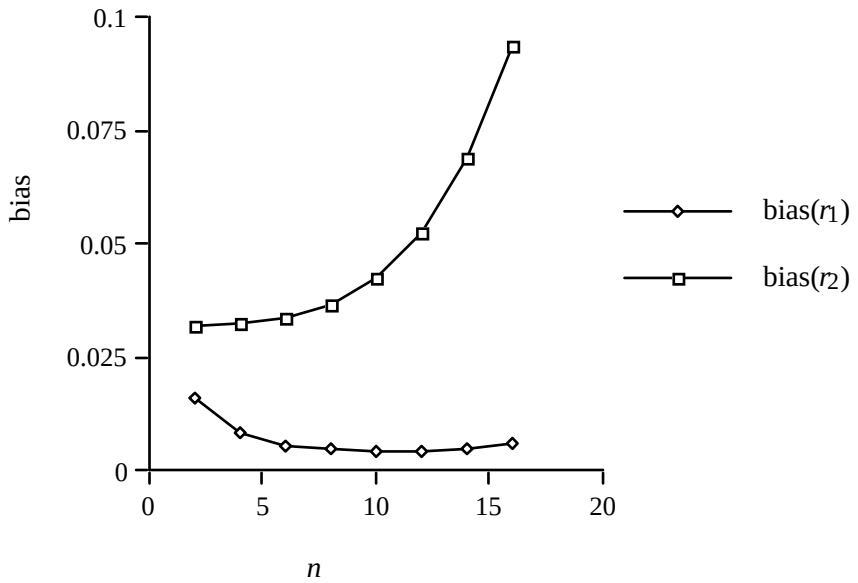

Figure 6. The bias terms of r_1 and r_2 and the correction term of r_3 as a function of the number of samples n. We start with 2 samples in the middle of the chromosome and extend (increase by 2) to both sides till the borders (n = 16) are reached.

6.2. *Ratio labeling*

Today's practice in molecular cytogenetics is to label a chromosome probes with a single fluorochrome. The number of probes one can use to detect different chromosomes or parts of chromosomes simultaneously, is therefore restricted by the number of fluorochromes that can be spectrally separated in fluorescence microscopy. In practice, only three fluorochromes can be used simultaneously, e.g. blue (DAPI), green (FITC), and red (TRITC, Texas Red). Spectral

extension into the UV poses optical problems and extensions into the IR prohibits the use of IR blocking filters in front of a CCD camera.

To increase the number of molecular probes that can be used simultaneously, one could label a probe with a combination of fluorochromes. However, the hybridization efficiency of fluorescently labeled probes is difficult to control [1]. Therefore the absolute intensity of the probe colors cannot be used to distinguish different probes. The ratio between the probe colors can be used to identify chromosome probes. Some experiments were performed to determine the variance and covariance of double labeled chromosome probes [1]. In these experiments the ratios were selected based on molecular concentrations. To apply the theory presented below for optimization of the selected ratios, the total efficiency of each fluorophore (labeling of fluorophore on a substrate, life-time, quantum efficiency, etc.) under certain conditions needs to be known.

The expressions for the mean and variance of ratio estimators are not very practical for this application. The ratio values of signals *a/b* and *b/a* are not symmetrical around 1 and even approach infinity if the denominator becomes zero. In this application, the use of polar coordinates *r* and φ is more intuitive. The ratio is determined by the angle φ and the absolute intensity of both signals by *r*. As mentioned, we cannot use the absolute intensity *r* to characterize the a chromosome probe. Therefore, we need to determine the mean and variance of the estimation of φ, given *x* and *y*, to determine the maximum number of ratio labels one can use for probes with two fluorochromes.

Similar to derivations in section 2, we have used a second order Taylor approximation of the arc tangent of *x* and *y* to derive the mean of φ given *x* and *y*,

$$\begin{aligned} \mathrm{E}\{\varphi|x,y\} &= \mathrm{E}\{\arctan(x/y)\} \\ &\approx \arctan\left(\mu_x/\mu_y\right) + \frac{\mu_x\mu_y(\operatorname{var} y - \operatorname{var} x) + \left(\mu_x - \mu_y\right)^2 \operatorname{cov}(x,y)}{\left(\mu_x^2 + \mu_y^2\right)^2} \end{aligned} \tag{16}$$

The variance of the estimation of φ is derived, using a first order Taylor approximation,

$$\begin{aligned} \operatorname{var}(\varphi|x,y) &= \mathrm{E}\left\{\left(\arctan(x/y) - \mathrm{E}\{\arctan(x/y)\}\right)^2\right\} \\ &\approx \frac{\mu_y^2 \operatorname{var} x + \mu_x^2 \operatorname{var} y - 2\mu_x\mu_y \operatorname{cov}(x,y)}{\left(\mu_x^2 + \mu_y^2\right)^2} \end{aligned} \tag{17}$$

To find the ratios (for a given number of labels) with the maximum separability one has to incorporate the variance of φ in the metric.

The theory for probes labeled with two fluorochromes can be extended to probes labeled with three fluorochromes. For three colors *x*, *y* and *z* we can use the ratio angles φ and θ

$$\varphi = \arctan(x/y) \qquad \theta = \arctan\left(z/\sqrt{x^2 + y^2}\right) \tag{18}$$

The ratio labels are in this case distributed on an octant of a sphere. The distance metric is determined by the variances of φ and θ. To find the maximum number of ratio labels, one has to find for every number of points the optimal distribution on the sphere and check whether the minimum distance between two ratios is large enough. With the optimal distribution on the sphere is meant the distribution for which the minimum distance between two points is maximized for a given metric.

7. Conclusion

In this paper we have derived expressions for the mean and variance of two intuitive manners to estimate the ratio between two random variables. We have shown that one of these estimators (r_2) is biased and that the other (r_1) is only asymptotically unbiased. For positive ratios, r_1 and r_2 will always overestimate the ratio. However, from the expression for the bias of r_1 we have derived an unbiased ratio estimator r_3. These results where supported by experiments. The noise data for these experiments was either computer generated or measured camera noise.

The Cramer Rao lower bound or minimum variance bound for unbiased ratio estimators was derived. The approximation of the variance of our unbiased estimator r_3 is equal to this lower bound for Gaussian distributed additive noise.

For a particular application of ratio imaging, CGH, we have shown that the usual averaging over multiple ratio profiles is not optimal. Measurements on CGH images confirms the differences between the ratio estimators, as found in the other experiments. Furthermore, we showed that the variance of the ratio estimators on these images were not dominated by the acquisition system, but due to variations in the biology or the hybridization procedure.

Acknowledgment

We thank Jim Piper , Joe Gray and Damir Sudar for given us a copy of their CGH images. This work was partially supported by The Netherlands Organization for Scientific Research (NWO) and the ASCI PostDoc program.

References

[1] P.M. Nederlof, *Methods for Quantitative and Multiple In Situ Hybridization,* (Ph.D. Thesis), Rijksuniversiteit te Leiden, 1991, Chapter 8.

[2] D. Shotton, *Electronic Light Microscopy,* Wiley-Liss, 1993, Chapter 8.

[3] A. Kallioniemi, O-P. Kallioniemi, D. Sudar, D. Rutovitz, J.W. Gray, F. Waldman and D. Pinkel, *Comparative Genome Hybridization for Molecular Cytogenetic Analysis of Solid Tumors,* Science 258, 1992, pp. 818-821

[4] J. Piper, D. Rutovitz, D. Sudar, A. Kallioniemi , O-P. Kallioniemi, F. Waldman, J.W. Gray and D. Pinkel, *Computer Image Analysis of Comparative Genomic Hybridization,* Cytometry, vol. 19, no. 1, 1995, pp. 10-26.

[5] Kendall and Stuart, *The Advanced Theory of Statistics,* vol 1, Charles Griffin & Company, 1977.

[6] W.H. Press, B.P. Flannery, S.A. Teukolsky, W.T. Vetterling, *Numerical Recipes in C,* Cambridge University Press, Cambridge U.K., 1988.

[7] J.C. Mullikin, L.J. van Vliet, H. Netten, F.R. Boddeke, G. van der Feltz and I.T. Young, *Methods for CCD Camera Characterization,* SPIE Vol. 2173, 1994, pp. 73-84.